

# Influence of crystallite size on the surface properties of calcium-deficient hydroxyapatites

Allal Barroug

Université Cadi Ayyad, Faculté des Sciences Semlalia, Bd Prince Moulay Abdellah, B.P.S. 15, Marrakech (Morocco)

Jacques Lemaître\*

Ecole Polytechnique Fédérale de Lausanne, Laboratoire de Technologie des Poudres, MX-Ecublens, CH-1015 Lausanne (Switzerland)

Paul G. Rouxhet

Université Catholique de Louvain, Unité de Chimie des Interfaces, Place Croix-du-Sud 2/18, B-1348 Louvain-la-Neuve (Belgium)

## Abstract

The surface properties of calcium-deficient hydroxyapatites (HAPs) prepared under different synthesis conditions (e.g. by precipitation at pH 10, or by hydrolysis of dicalcium phosphate at pH 6.5) were studied. All the products tested were pure, well crystallized calcium-deficient HAPs. The samples prepared under slightly acidic conditions exhibit larger crystallite sizes and higher calcium deficiency compared with those prepared under alkaline conditions.

Electrophoretic mobilities were measured as a function of pH in  $1.0 \times 10^{-3}$  M  $\text{KNO}_3$  aqueous solutions. The isoelectric points (iep) of HAP appear to depend strongly on the synthesis conditions; iep values of 4 were found for samples prepared under more acidic conditions, while values ranging from 5.5 to 7.2 were found for solids precipitated from alkaline solutions.

The adsorption of hen egg-white lysozyme was measured at ambient temperature, in  $1.0 \times 10^{-3}$  M  $\text{KNO}_3$  aqueous solutions buffered at pH 6.8 with  $2.0 \times 10^{-3}$  M phosphate buffer. The parameters of the Langmuir-type adsorption isotherms were found to depend significantly on the specific surface of the samples; the monolayer coverage goes through a maximum of  $40 \times 10^{-9}$  mol  $\text{m}^{-2}$  at  $S_{\text{BET}} = 80 \text{ m}^2 \text{ g}^{-1}$ , while the affinity constant culminates at  $355 \text{ mM}^{-1}$  at the same value of  $S_{\text{BET}}$ . The decay of both monolayer coverage and affinity constant beyond  $S_{\text{BET}} = 80 \text{ m}^2 \text{ g}^{-1}$  can be ascribed partly to the lower accessibility of smaller pores to lysozyme molecules, particularly when electrostatic repulsion exists between the lysozyme molecules and the HAP surface. It is thought that specific bonds between lysozyme and the hydroxyapatite surface must exist, which are very sensitive to the nature and the relative amounts of crystallographic planes exposed on the solid surface.

## 1. Introduction

Several electrochemical studies of the synthetic apatite–aqueous solution interface have been undertaken to throw light on the mechanisms governing their adsorption properties and their flotability [1–4].

The influence of the composition of the adsorbing solution on the surface charge and the adsorptive properties of various synthetic hydroxyapatites for hen egg-white lysozyme has been reported [1]. The adsorption mechanism is controlled by electrostatic interactions between adsorbate and adsorbent, and is consistent with a fast and reversible surface neutralization process.

The present contribution reports some effects of the microstructural characteristics of synthetic calcium-deficient hydroxyapatites on their electrokinetic and adsorption properties.

## 2. Experimental details

Hydroxyapatite HAP-I, referred to in a previous work as HAP-IA [1] was prepared by the progressive addition during 3 h of a calcium nitrate solution into an ammonium phosphate solution at  $80^\circ\text{C}$  at a pH close to 10. Full details of the precipitation technique are reported elsewhere [5]. Samples HAP-IIA and HAP-IIB were obtained by slow hydrolysis in the presence of urea of anhydrous dicalcium phosphate at  $90^\circ\text{C}$ , and dicalcium phosphate dihydrate at  $80^\circ\text{C}$  respectively. The procedure is reported in full detail elsewhere [6, 7]. Sample HAP-III is a commercial material (Bio-Gel HTP, Biorad Laboratories) sold as a support for liquid phase chromatography. Its preparation process is reported elsewhere [8]; it includes a controlled precipitation under alkaline conditions.

The adsorbate used for this study was a commercial hen egg-white lysozyme supplied by Sigma (N6876 Grade 1).

\*Author to whom correspondence should be addressed.

The solid materials were characterized by X-ray diffraction (Philips, Norelco diffractometer PW 1130, Cu K $\alpha$  radiation), temperature programmed reaction [6], IR spectroscopy (Beckman IR 12 spectrometer), transmission electron microscopy (AEI, type EM6G microscope), mercury intrusion porosimetry (Carlo Erba 200 porosimeter) and elemental analysis [9]. The specific surfaces were determined by the BET method, using nitrogen adsorption measurements at the boiling temperature of nitrogen.

The electrophoretic mobilities of the samples were determined with a Pen Kem 500 Laser-Zee meter, equipped with a standard poly(methyl methacrylate) cell. Aqueous KNO<sub>3</sub> 1.0  $\times$  10<sup>-3</sup> M solutions were used as suspension media. The pH was adjusted to the desired value using either HNO<sub>3</sub> or KOH 1.0  $\times$  10<sup>-4</sup> M solutions. 20 mg of the solid was mixed with 100 ml of the solution and equilibrated for 24 h at ambient temperature under continuous stirring.

Adsorption experiments were performed as follows. The desired amount of adsorbent (100 mg, unless otherwise stated) was suspended in 9 ml of a KNO<sub>3</sub> 1.0  $\times$  10<sup>-3</sup> M solution buffered at pH 6.8 (2.0  $\times$  10<sup>-3</sup> M phosphate buffer); a portion of the desired lysozyme solution (1 ml) was then added to the adsorbent suspension. Lysozyme concentrations were chosen in the range 0.05–2.00 g l<sup>-1</sup>. The mixture was equilibrated for 3 h at ambient temperature under continuous stirring. The residual lysozyme concentration was determined by measuring the absorbance at 282 nm, using a UV-visible spectrophotometer (Beckman ACTA M IV) [10].

### 3. Results and discussion

All the samples presented below exhibit the X-ray diffraction patterns and IR spectra characteristic of pure and well crystallized hydroxyapatites. The chemical analyses (Table 1) show that the samples are calcium deficient hydroxyapatites ([Ca]/[P] atomic ratio less than 1.67). In addition to the characteristic bands of OH<sup>-</sup> (3560 cm<sup>-1</sup>) and PO<sub>4</sub><sup>3-</sup> groups (bands at 1010–

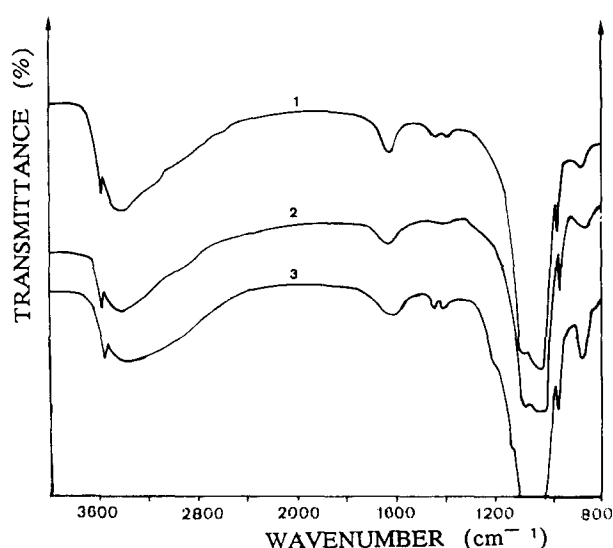


Fig. 1. IR spectra of hydroxyapatites: (1) HAP-I, (2) HAP-III and (3) HAP-IIA.

1110 cm<sup>-1</sup>), the IR spectra show (Fig. 1) the presence of HPO<sub>4</sub><sup>2-</sup> groups (bands at 875 and 1180–1200 cm<sup>-1</sup>), and traces of carbonates (bands at 1410 and 1450 cm<sup>-1</sup>), pointing to non-stoichiometric compounds [11]. The samples prepared under slightly acidic conditions (HAP-IIA and HAP-IIB) exhibit much stronger HPO<sub>4</sub><sup>2-</sup> bands compared with those precipitated under alkaline conditions (HAP-I and HAP-III).

Figure 2 shows how the morphology of the precipitated crystals is affected by the synthesis conditions. Thus, slow hydrolysis (HAP-IIA and HAP-IIB) results in the formation of acicular crystals, 0.2–17  $\mu$ m in length, very similar to those obtained through the hydrolysis of tricalcium phosphate [12]. Specimens obtained by fast precipitation (HAP-I and HAP-III) consist of agglomerates of small crystallites, 0.1–0.2  $\mu$ m in length. The specific surface area of the specimens ranges from 5 up to 123 m<sup>2</sup> g<sup>-1</sup> (Table 1), well within the 25–200 m<sup>2</sup> g<sup>-1</sup> range reported previously by Holmes *et al.* [13]. The pore radii  $R_{50}$ , corresponding to a cumulated pore surface of 50% of the total specific

TABLE 1. Chemical analysis and microstructural characteristics of hydroxyapatite samples

Sample	[Ca]/[P] atomic ratio	BET surface (m <sup>2</sup> g <sup>-1</sup> )	$R_{50}$ <sup>a</sup> (nm)	Particle size ( $\mu$ m)
HAP-I	1.58	123	18	0.1–0.2
HAP-IIA	1.55	5	500	0.4–17
HAP-IIB	1.56	43	30	0.2–1.6
HAP-III	1.50	80	8	0.1–0.2

The general formula of calcium-deficient hydroxyapatite is Ca<sub>10-x</sub>(HPO<sub>4</sub>)<sub>2x</sub>(PO<sub>4</sub>)<sub>6-x</sub>(OH)<sub>2</sub>, where  $x$  is related to the [Ca]/[P] atomic ratio by  $x = 10 - 6([Ca]/[P])$ .

<sup>a</sup>The cumulated surface of pores with radii less than  $R_{50}$  corresponds to 50% of the total surface area.

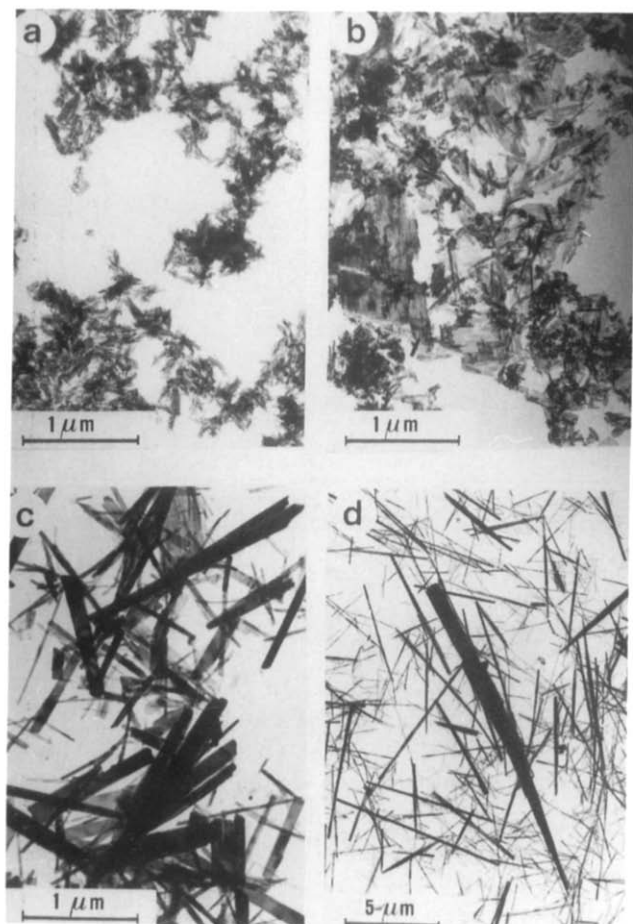


Fig. 2. Transmission electron microscopy of synthetic hydroxyapatite samples: (a) HAP-I, (b) HAP-III, (c) HAP-IIB and (d) HAP-IIA.

surface area of the samples, were deduced from pore size distribution measurements, assuming open cylindrical pores. All the samples exhibit  $R_{50}$  lower than 30 nm, except sample HAP-IIA for which  $R_{50} = 500$  nm.

Figure 3 presents the effect of pH on the electrophoretic mobility of the samples, in  $1.0 \times 10^{-3}$  M  $\text{KNO}_3$  aqueous solutions. The isoelectric points (iep) are presented in Table 2. The samples prepared under alkaline conditions (HAP-I and HAP-III) exhibit the highest iep values (7.2 and 5.5 respectively), while those prepared under more acidic conditions (HAP-IIA and HAP-II-B) have significantly lower iep values (3.8–4.0). These observations agree well with literature data: Arends [14] reports that the Bio-Gel HTP apatite is negatively charged beyond pH 5.5–6.0, and more negatively charged under similar conditions than another commercial stoichiometric apatite ( $[\text{Ca}]/[\text{P}] = 1.63$ , Merck HTP); other authors [2, 4] report iep values of 6.5 and 7.4 for hydroxyapatites with  $[\text{Ca}]/[\text{P}] = 1.61$  and 1.59 respectively. Lowering of the iep of synthetic hydroxyapatites from 8.5 to 6.8 in the presence of  $\text{Na}^+$

TABLE 2. Isoelectric points and parameters of the Langmuir adsorption isotherms of lysozyme on hydroxyapatite samples

Sample	Isoelectric point	$N^a$ ( $\text{nmol m}^{-2}$ )	$K^a$ ( $\text{mM}^{-1}$ )
HAP-I	7.2	$22.3 \pm 1.5$	$228 \pm 40$
HAP-IIA <sup>b</sup>	3.8	< 17	—
HAP-IIB	4.0	$35.0 \pm 9.0$	$29 \pm 16$
HAP-III	5.5	$41.0 \pm 2.0$	$356 \pm 45$

<sup>a</sup>Maximum adsorbable amount  $N$  and affinity constant  $K \pm 95\%$  confidence interval.

<sup>b</sup>75  $\text{g l}^{-1}$  in suspension.

or  $\text{F}^-$  ions has also been reported [15]. The comparatively lower iep found in this study for the samples prepared at lower pH cannot be explained by compositional differences of the contact solutions. Indeed, all the solutions used here presented identical concentrations in calcium and phosphate ions, which are known to be the main potential determining ions [1]. Summarizing these results, although uncontrolled effects of impurities cannot be completely discarded, higher  $[\text{Ca}]/[\text{P}]$  ratios and higher pH of the mother solutions are thought to be the main factors contributing to the increased iep of hydroxyapatites.

Lysozyme adsorption isotherms on apatites are of the Langmuir type. The parameters of the isotherms were determined by linear regression, using the following linearized equation [1]:

$$Q = N - Q/KC$$

where  $Q$  ( $\text{mol m}^{-2}$ ) is the amount of adsorbed protein per unit surface of adsorbent,  $C$  ( $\text{mol l}^{-1}$ ) is the equilibrium adsorbate concentration,  $N$  ( $\text{mol m}^{-2}$ ) is the maximum

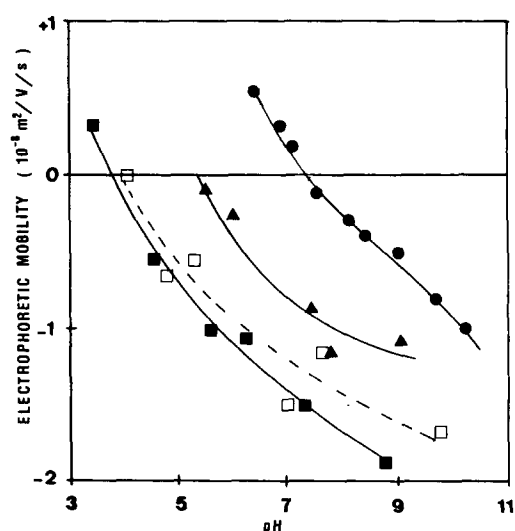


Fig. 3. Electrophoretic mobility vs. pH of hydroxyapatites suspended in  $1.0 \times 10^{-3}$  M  $\text{KNO}_3$  solutions: (●) HAP-I, (■) HAP-IIA, (□) HAP-IIB and (▲) HAP-III.

adsorbable amount of protein and  $K$  ( $1 \text{ mol}^{-1}$ ) is the affinity constant of the protein for the adsorbing surface. The results are summarized in Table 2.

A plot of the Langmuir parameters *vs.* the BET surface of the samples is shown in Fig. 4. The largest amount of lysozyme is adsorbed by sample HAP-III, which also exhibits the highest affinity constant, followed by samples HAP-IIB and HAP-I. Sample HAP-IIA exhibits no measurable affinity for lysozyme. Figure 4 shows that the maximum adsorbable amount  $N$  and the affinity of lysozyme  $K$  initially increase with the BET surface of the adsorbents, going through a maximum at  $S_{\text{BET}} = 80 \text{ m}^2 \text{ g}^{-1}$ . With the exception of sample HAP-I, which is discussed later separately, a systematic trend thus appears: higher  $N$  and  $K$  values are associated with higher specific surfaces and smaller pore radii. This observation suggests that higher surface concentrations of more energetic adsorption sites exist on smaller HAp crystals, or inside narrower pores. However, inspection of Fig. 3 shows that lower negative surface charges at the adsorption pH (6.8) are found for samples having higher affinities for lysozyme; this is the opposite of what would be anticipated if the adsorption process were governed by electrostatic interactions alone, for more negative surfaces would then be expected to attract more strongly the positively charged lysozyme molecules. This points to a specific adsorption mechanism, in which electrostatic interactions only play a minor role. This is not to say that electrostatic interactions do not play any role at all, and this is probably well illustrated by the case of HAP-I, for which values of  $N$  and  $K$  are markedly lower than expected on the basis of the general trends discussed above. Figure 3 shows that sample HAP-I is positively charged at the adsorption pH (6.8). Hence, the positively charged lysozyme molecules must jump over an

electrostatic activation barrier before they can adsorb onto the HAp surface. Owing to higher space charge concentrations, electrostatic repulsion is likely to be stronger in the pores, the more so as the pore radius becomes smaller. As a consequence, the smallest pores can become completely inaccessible to the lysozyme molecules. The surface fraction available for adsorption will decrease accordingly, resulting in a decreased average monolayer coverage.

#### 4. Conclusions

This work has shown that lysozyme adsorbs on hydroxyapatite according to a mechanism involving specific adsorption sites, by which surface concentration and affinity seem to increase together with the specific surface of the adsorbent. Electrostatic interactions are of minor importance, except when HAp is positively charged. In that case, electrostatic repulsion can prevent positively charged lysozyme molecules from accessing the HAp surface exposed in the smallest pores. The synthesis conditions, including pH, temperature and time, clearly play a crucial role in determining not only the degree of calcium deficiency and the iep, but also the microstructural characteristics of the hydroxyapatite such as crystal morphology and size, the latter affecting globally the specific surface and pore size distribution of the samples.

It can be anticipated that, if lysozyme is to adsorb on specific sites at the surface of hydroxyapatite, the extent of adsorption must be sensitive to the nature and relative amounts of crystal facets exposed by the adsorbing solid. Systematic work on a larger variety of carefully prepared hydroxyapatites should be undertaken in order to elucidate the nature of the crystallographic planes favourable to lysozyme adsorption. Observations of the extent of lysozyme adsorption on different facets of hydroxyapatite monocrystals, synthesized under hydrothermal conditions, are already in progress [16].

#### Acknowledgments

The financial support of "Service de Programmation de la Politique Scientifique" (Concerted Action in Physical Chemistry of Interface and Biotechnology, Belgium) is gratefully acknowledged.

#### References

- 1 A. Barroug, J. Lemaître and P. G. Rouxhet, *Colloids Surf.*, 37 (1989) 339.

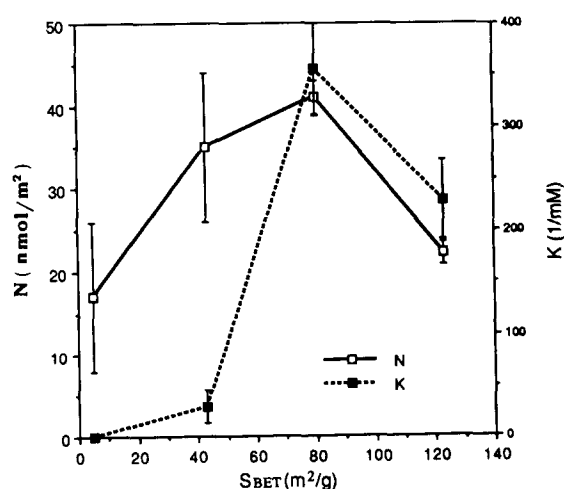


Fig. 4. Influence of the BET specific surface of hydroxyapatites on the parameters of their Langmuir adsorption isotherms.

- 2 R. K. Mishra, C. Chander and D. W. Fuerstenau, *Colloids Surf.*, 1 (1980) 105.
- 3 P. Somasundaran and Y. H. C. Wang, in D. N. Mistra (ed.), *Adsorption on and Surface Chemistry of Hydroxyapatite*, Plenum, New York, 1984, p. 129.
- 4 J. Ofori Amankonah and P. Somasundaran, *Colloids Surf.*, 15 (1985) 335.
- 5 A. Barroug, *3rd Cycle Thesis*, Institut National Polytechnique, Toulouse, France, 1982.
- 6 A. Mortier, J. Lemaître, L. Rodrique and P. G. Rouxhet, *J. Solid State Chem.*, 78 (1989) 215.
- 7 A. Mortier, J. Lemaître and P. G. Rouxhet, *Thermochim. Acta*, 143 (1989) 265.
- 8 A. Tiselius, S. Hjerten and O. Levin, *Arch. Biochem. Biophys.*, 65 (1956) 132.
- 9 G. Charlot, *Les Méthodes de la Chimie Analytique*, Masson, Paris, 1960, p. 1023.
- 10 A. Barroug, *PhD Thesis*, Université Catholique, Louvain-la-Neuve, Belgium, 1989.
- 11 J. C. Heughebaert, *PhD Thesis*, Institut National Polytechnique, Toulouse, France, 1977.
- 12 C. Rey, *PhD Thesis*, Institut National Polytechnique, Toulouse, France, 1984.
- 13 J. M. Holmes, R. A. Beebe, A. S. Posner and R. A. Harper, *Proc. Soc. Exper. Biol. Med.*, 133 (1970) 1250.
- 14 J. Arends, *J. Dent.*, 7 (1979) 246.
- 15 L. C. Bell, A. M. Posner and J. P. Quirk, *Nature (London)*, 239 (1972) 515.
- 16 G. Vereecke, J. Arends and P. G. Rouxhet, unpublished results.